Acta Crystallographica Section D
**Biological Crystallography**
ISSN 0907-4449

# Selective X-ray-induced NO photodissociation in haemoglobin crystals: evidence from a Raman-assisted crystallographic study

**Antonello Merlino,[a,b] Martin R. Fuchs,[c] Andrea Pica,[a] Anna Balsamo,[a] Florian S. N. Dworkowski,[c] Guillaume Pompidor,[c] Lelio Mazzarella[a] and Alessandro Vergara[a,b]***

[a]Department of Chemical Sciences, University of Naples 'Federico II', Via Cintia, I-80126 Naples, Italy, [b]Istituto di Biostrutture e Bioimmagini, CNR, Naples, Italy, and [c]Swiss Light Source, Paul Scherrer Institute, Villigen, Switzerland

Correspondence e-mail: avergara@unina.it

Received 24 July 2012
Accepted 9 October 2012

Despite their high physiological relevance, haemoglobin crystal structures with NO bound to haem constitute less than 1% of the total ligated haemoglobins (Hbs) deposited in the Protein Data Bank. The major difficulty in obtaining NO-ligated Hbs is most likely to be related to the oxidative denitrosylation caused by the high reactivity of the nitrosylated species with $O_2$. Here, using Raman-assisted X-ray crystallography, it is shown that under X-ray exposure (at four different radiation doses) crystals of nitrosylated haemoglobin from *Trematomus bernacchii* undergo a transition, mainly in the $\beta$ chains, that generates a pentacoordinate species owing to photodissociation of the Fe—NO bond. These data provide a physical explanation for the low number of nitrosylated Hb structures available in the literature.

## 1. Introduction

Nitrogen monoxide (NO) is a signalling molecule involved in the regulation of essential physiological processes (Moncada *et al.*, 1991). Endogenous NO is produced by metabolism of L-arginine catalyzed by the enzyme NO synthetase (with haem as a co-enzyme) and by the nitrite reductase activity of deoxy hemoglobin (Hb). Thus, there is great interest in understanding the NO–haem interaction, which is of tremendous physiological importance and is vital to a number of biological processes, including neurotransmission, vasodilation and blood clotting. The interaction between NO and haemoproteins is relevant to all of these processes, with many iron-containing proteins being modulated *in vivo* by NO (Bonaventura *et al.*, 2004; Chan *et al.*, 1998). The molecular mechanisms of many of these interrelated biochemical pathways are still controversial (Moncada *et al.*, 1991).

Reactivity of NO with Hbs has been shown both at the haem and the cysteine residues (Chan *et al.*, 1998). However, NO and related reactive species also react with other amino-acid residues, such as Tyr (Martínez-Ruiz *et al.*, 2011) and Trp (Suntsova *et al.*, 2002). Moreover, NO-mediated chemical modification of amino-acid residues may affect the reactivity of the haem. Crystal structures of human Hb (HbA) *S*-nitrosylated at Cys93$\beta$ (Chan *et al.*, 1998) and with NO bound at the haem iron (Chan *et al.*, 2004) are both available. The study of such nitrosylated species is complicated by the high reactivity of haem–NO complexes, which undergo rapid oxidative denitrosylation under aerobic conditions. The nitrosylated Hb structures available in the literature were obtained *via* NO soaking into deoxygenated HbA crystals (Chan *et al.*, 2004). The crystal structure of the fully liganded T-state complex of HbA with NO revealed the striking and surprising result that the bond between the haem iron and the proximal histidine in the $\alpha$ subunits is ruptured (Chan *et al.*, 2004). This finding is in good agreement with the resonance Raman (Szabo & Barron, 1975) and infrared (Maxwell & Caughey, 1976) spectra, which exhibit a mixture of pentacoordinated and hexacoordinated NO adducts. In contrast, in the $\beta$ subunits the iron–proximal histidine bond is intact. It is also known that visible laser-induced photodissociation can be a minor source of denitrosylation, but with very low quantum yields in the visible region (Opisov *et al.*, 2007).

Here, we present an additional experiment-generated source of denitrosylation owing to X-ray photolysis of crystals of nitrosylated Hb from the Antarctic fish *Trematomus bernacchii* (HbTb). Crystal structures of HbTb are available in several ferrous (Camardella *et al.*, 1992; Mazzarella *et al.*, 2006) and ferric forms (Vergara *et al.*, 2007, 2009; Merlino *et al.*, 2011) at different pH values. Indeed, this system represents a model for the study of the peculiarities of fish Hb [such as the Root effect (Verde *et al.*, 2008) and haemichrome formation (Verde *et al.*, 2008; Vitagliano *et al.*, 2008; Merlino *et al.*, 2011)].

X-ray-induced radiation damage is a frequent phenomenon, especially when third-generation synchrotrons are used. Several examples of photo-damage to protein side chains have been reported (Garman, 2010; Murray *et al.*, 2004). Raman microscopy prior to and after X-ray data collection can be a valuable tool for the detection of such artifacts. Indeed, several papers on Raman-assisted crystallographic studies have recently been published; these include, as examples, Br dissociation from DNA (McGeehan *et al.*, 2007) and disulfide reduction (Carpentier *et al.*, 2010). Very recently, X-ray-induced NO photodissociation at low temperature was reported for HbA in solution *via* XANES studies (Arcovito & Della Longa, 2011). However, to the best of our knowledge this is the first Raman-assisted crystallographic evidence for X-ray-induced NO photodissociation at a third-generation synchrotron (the Swiss Light Source). Indeed, the Raman spectra of the X-ray-exposed single crystals showed NO photodissociation that electron-density maps revealed to be localized mainly in the $\beta$ subunits. Ultimately, our combined crystallographic and spectroscopic method has provided (i) an experimental protocol for the detection of X-ray-induced NO photodissociation in haemoprotein crystals *via* Raman microscopy and (ii) a method to obtain approximate quantitative information on the relative Raman cross-section of the bands corresponding to deoxygenated and nitrosylated Hbs. This latter result may be useful to quantitatively evaluate the degree of NO photodissociation in future studies and as a reference for computational studies on resonance Raman (RR) spectra.

## 2. Methods

### 2.1. Crystallization of NO-bound haemoglobin

Deoxygenated HbTb crystals at pH 6 were produced as reported previously (Mazzarella *et al.*, 2006). Nitrosylation was achieved just prior to X-ray data collection *via* NO soaking of deoxygenated crystals. NO was produced *in situ* by adding a degassed equimolar solution of sodium dithionite and sodium nitrite (30 m*M*). The soaking time (15 min) was defined *via* off-line Raman microscopy (see below).

### 2.2. Raman microscopy

**2.2.1. Off-line Raman microscopy**. In order to define the experimental nitrosylation protocol, preliminary RR microscopy spectra were collected from HbTb deoxy crystals in the Department of Chemical Sciences at University of Naples 'Federico II' using an apparatus described elsewhere (Vergara, Merlino *et al.*, 2008). The excitation line was 514 nm ($Ar^+$ laser), with a power of 2 mW at the sample.

**2.2.2. Online Raman microscopy**. Prior to and after each collection of X-ray diffraction data, RR spectra were collected on beamline X10SA of the Swiss Light Source (SLS) using an upgraded version of the microspectrophotometer previously reported (Owen *et al.*, 2009). RR spectra were collected from a crystal that was maintained in the same orientation. The excitation wavelength was 405 nm (Omicron LDM405.400 diode laser) with a power at the sample of 5 mW in a 50 µm round focal spot. Successive RR spectra were collected to rule out the occurrence of significant photodissociation upon laser exposure. Indeed, no detectable difference was observed in such successive RR spectrum (data not shown), as reported in the literature (Opisov *et al.*, 2007).

### 2.3. X-ray data collection

Diffraction data were initially collected in-house using a Rigaku MicroMax-007 HF X-ray generator equipped with a Saturn944 CCD detector and a copper rotating-anode source. Using this conventional source, the resolution limit was 2.0 Å (data not shown). Diffraction data for fully (NO-HbTb) and partially (NO_x1-HbTb, NO_x2-HbTb and NO_x3-HbTb) nitrosylated HbTb crystals were collected on beamline X10SA of the SLS at four different X-ray doses. X-ray diffraction data for NO_x1-HbTb, NO_x2-HbTb and NO_x3-HbTb were collected from the same crystal. Results similar to those described for NO-HbTb were obtained using a different crystal (NO-HbTb-bis). Data-collection statistics are reported in Supplementary Table S1.[1] All data sets were collected at 100 K using glycerol as a cryoprotectant and were processed with the *HKL*-2000 program suite (v.7.01; Otwinowski & Minor, 1997). An analysis of the collected diffraction data showed that the NO-HbTb crystals present pseudo-merohedral twinning. This finding is in line with the previous results on deoxy crystals of the same Hb (Mazzarella *et al.*, 2006). The twin fractions, as determined by the algorithm implemented in the program *SHELX* (Sheldrick, 2008), were close to 0.5 in all cases. The refinements were performed with *SHELX* (Sheldrick, 2008). The structures refined to the $R$ factor and $R_{\rm free}$ values reported in Suppementary Table S1. Further structural details will be reported elsewhere. The X-ray dose was evaluated using the software *RADDOSE* (Paithankar *et al.*, 2009). Owing to the large number of frames and the long exposure time used for in-house experiments, the total X-ray dose was comparable with that of the synchrotron X-ray data collection. The structure of NO-HbTb has been deposited in the Protein Data Bank as entry 4g51.

## 3. Results and discussion

The in-house NO soaking of deoxygenated HbTb crystals at pH 6 was monitored *via* Raman microscopy with excitation at 514 nm (Supplementary Fig. S1). The best conditions to obtain a fully nitrosylated form were 30 m*M* sodium dithionite, 20 m*M* sodium nitrite with a 10 min soaking time. Soaking experiments were highly reproducible when degassed solutions and a reducing environment were used. NO formation was monitored by following the position and the intensity of Raman bands, which change from values typical of the deoxy form ($\nu_4$ = 1355 and $\nu_2$ = 1375 $cm^{-1}$; Kitagawa *et al.*, 1978; Spiro & Strekas, 1974) to those typical of the nitrosylated form ($\nu_4$ = 1370, $\nu_2$ = 1505 and $\nu_{10}$ = 1635 $cm^{-1}$; Stong *et al.*, 1980). The fully ligated form was also analyzed at higher spectral resolution in order to evaluate the NO coordination (Supplementary Fig. S1). The $\nu_{10}$ value of 1635 $cm^{-1}$ revealed the presence of hexacoordinated HbTb. No detectable bands for the pentacoordinated nitrosylated species, the $\nu_{10}$ of which would be expected to be at 1640 $cm^{-1}$ (Szabo & Barron, 1975), were observed. This finding indicates differing behaviour between HbA and HbTb. Interestingly, the absence of the pentacoordinated species seems to be a common feature of fish Hbs,

[1] Supplementary material has been deposited in the IUCr electronic archive (Reference: DW5025). Services for accessing this material are described at the back of the journal.

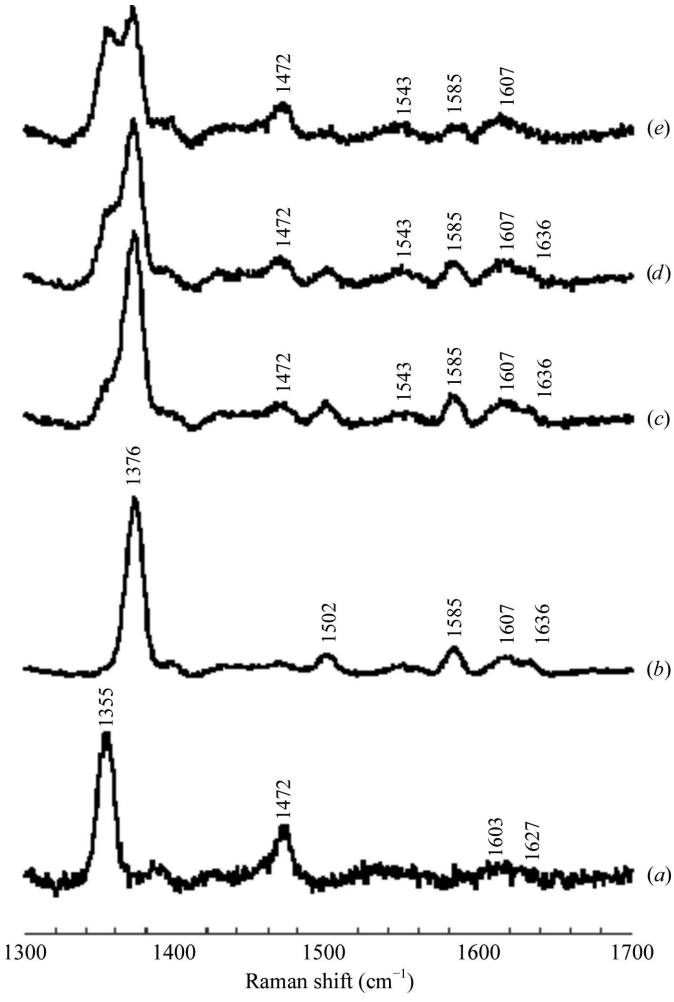


**Figure 1**
Resonance Raman spectra of HbTb crystals in the deoxygenated form (*a*), the fully nitrosylated form (NO-HbTb) (*b*) and the partially ligated forms NO_x1-HbTb (*c*), NO_x2-HbTb (*d*) and NO_x3-HbTb (*e*) arising from X-ray exposure at three different doses: 4.0, 7.6 and 11.2 MGy, respectively. The excitation line is 405 nm (5 mW at the sample) and the exposure time is 300 s. The spectral resolution is 8 $cm^{-1}$.

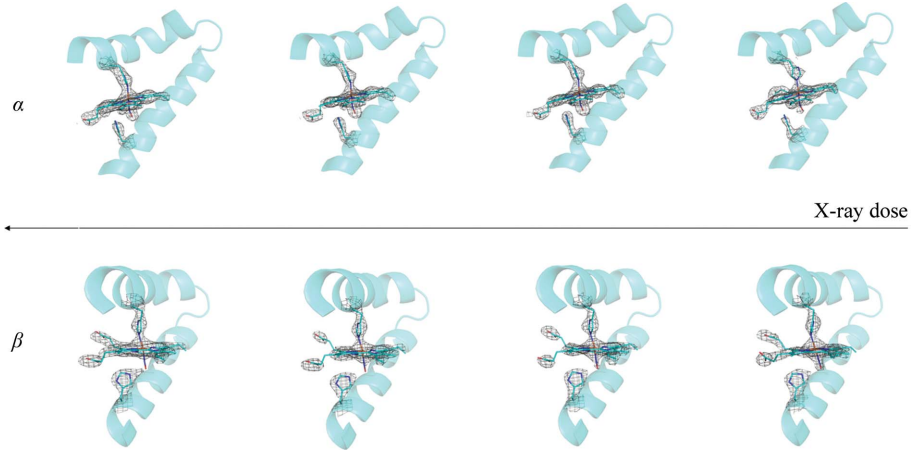


**Figure 2**
Difference Fourier electron-density maps ($2F_o - F_c$) of the $\alpha_1$ and $\beta_1$ haems of NO-HbTb and partially ligated forms (NO_x1-HbTb, NO_x2-HbTb and NO_x3-HbTb) at different X-ray doses (0.4, 4.0, 7.6 and 11.2 MGy, respectively). The maps were prepared using data at the same resolution (2.5 Å) and at the same electron-density level (1.0$\sigma$).

since carp Hb also lacks the spectral characteristics typical of the pentacoordinated species (Scholler *et al.*, 1979).

Despite the reproducibility of the soaking protocol, which was monitored *via* RR, several in-house X-ray diffraction data collections using a wavelength of 1.54 Å only resulted in partial NO coordination limited to the $\alpha$ subunits (data not shown). Since oxidative denitrosylation was presumed, a protective environment (a mixture of ascorbate and catalase) was used. Even under these oxygen-free conditions, only partial binding was again obtained.

Simultaneous X-ray data collection assisted by online Raman spectroscopy prior to and after data collection at the SLS synchrotron (using a 1 Å wavelength) solved the puzzle. Indeed, RR data (with excitation at 405 nm) at the SLS prior to X-ray exposure showed complete binding of NO to haem prior to the diffraction experiment (Fig. 1), as revealed by $\nu_4$ and $\nu_3$ bands typical of hexacoordinated NO haemoglobin. The RR data collected at increasing X-ray doses revealed a detectable decrease in the low-spin (LS) signal and the appearance of a new high-spin (HS) signal. In particular, the X-ray exposure produced an almost 50% decrease in the NO band in favour of the deoxygenated form. Therefore, the RR data clearly showed an X-ray-induced NO photodissociation. Moreover, no additional bands that could be associated with a transient tetracoordinate haem (with NO and both proximal and distal His not bound to iron), as disputed for HbA (Arcovito & Della Longa, 2011), were observed in the HbTb RR spectra.

The spectroscopic data correlate well with the crystallographic evidence. No evidence of NO binding to Cys, Tyr and Trp residues was apparent (data not shown); therefore, we will focus on the haem pockets. $2F_o - F_c$ electron-density maps of the $\alpha_1$ and $\beta_1$ chains of fully ligated NO-HbTb refined at the moderate resolution of 2.5 Å are shown in Fig. 2. A comparison of these maps and those calculated from the structures refined using data collected at increasing X-ray doses provides a clear interpretation of the changing intensity of the NO signal (Fig. 2). Indeed, it is evident that NO photodissociation occurs to different degrees in the $\alpha$ and $\beta$ subunits (Fig. 2). In particular, NO photodissociation is almost confined to the $\beta$ haems (Fig. 2). The electron density of the NO molecule is already very poor in the $\beta_2$ haem in fully ligated NO-HbTb and in the $\alpha_2$ haem of NO_x3-HbTb. In order to make the comparison between the Raman data and the crystallographic data as consistent as possible, the occupancy factors of NO were estimated in the different structures and are reported in Table 1 together with the X-ray dose used for the corresponding data collection and the ratio between the intensity of the $\nu_4$ or $\nu_2$ bands corresponding to the NO and deoxygenated species. This strong heterogeneity between the $\alpha$ and $\beta$ haems is a well known phenomenon both in ferric (Vergara, Vitagliano *et al.*, 2008; Balsamo *et al.*, 2012) and deoxy fish Hbs (Vergara *et al.*, 2010).

NO photodissociation is probably a source of denitrosylation in all globins. Indeed, recent solution studies have revealed X-ray-induced photodissociation of NO in HbA at low temperature (Arcovito & Della Longa, 2011). The only available NO-bound structure of HbA was collected at moderate resolution (at low X-ray dose) and at room temperature (Chan *et al.*, 1998). Therefore, our Raman microscopic evidence of NO photodissociation for Hb from

**Table 1**
Estimated occupancy factors and relative intensities of some Raman bands for the photodissociated and nitrosylated species.

| | Total dose (MGy) | NO occupancy ($\alpha_1$, $\beta_1$, $\alpha_2$, $\beta_2$) | $I_{1355}/I_{1370}$ | $I_{1475}/I_{1505}$ |
|---|---|---|---|---|
| HbTb-NO | 0.4 | 1.0, 1.0, 1.0, 0.7† | 0 | 0 |
| NO_x1-HbTb | 4.0 | 1.0, 0.8, 1.0, 0.7 | 0.2 | 1.2 |
| NO_x2-HbTb | 7.6 | 1.0, 0.6, 1.0, 0.6 | 0.6 | 1.3 |
| NO_x3-HbTb | 11.2 | 1.0, 0.4, 0.4, 0.4 | 0.8 | 2.8 |

† The electron density of HbTb-NO is very poor in the $\beta_2$ chain.

*T. bernacchii* may have a general impact, since it may explain the surprisingly small number of crystal structures of nitrosyl Hbs deposited in the PDB. Indeed, while only a limited number of literature sources report the absence of the expected NO bound to the haemoprotein structure (Forouhar *et al.*, 2007), an unpredictably large number of unpublished data could be retained in scientists' drawers as negative observations. The methodological take-home message of this work is the advice to monitor NO binding *via* Raman microscopy prior to and after X-ray diffraction data collection, while keeping the dose as low as possible. Finally, it is worth noting that data such as those reported in Table 1 (relative Raman intensities and occupancy factors) collected at the same crystal orientation can provide relative resonance Raman cross-sections of different coordination states. However, this evaluation does require that the orientation dependence of the modes belonging to the different coordination states is identical. It is worth mentioning that calculations of resonance Raman spectra are still considered to be a formidable task (Santoro *et al.*, 2011) and this type of spectroscopic and structural data represent valuable input data for a current challenge in computational chemistry.

PNRA is acknowledged for financial support. SLS is acknowledged for travel grants to AM and AV. Umberto Oreste is acknowledged for providing *T. bernacchii* haemolysate.

## References


Arcovito, A. & Della Longa, S. (2011). *Inorg. Chem.* **50**, 9423–9429.
Balsamo, A., Sannino, F., Merlino, A., Parrilli, E., Tutino, M. L., Mazzarella, L. & Vergara, A. (2012). *Biochimie*, **94**, 953–960.
Bonaventura, C., Fago, A., Henkens, R. & Crumbliss, A. L. (2004). *Antioxid. Redox Signal.* **6**, 979–991.
Camardella, L., Caruso, C., D'Avino, R., di Prisco, G., Rutigliano, B., Tamburrini, M., Fermi, G. & Perutz, M. F. (1992). *J. Mol. Biol.* **224**, 449–460.
Carpentier, P., Royant, A., Weik, M. & Bourgeois, D. (2010). *Structure*, **18**, 1410–1419.
Chan, N.-L., Kavanaugh, J. S., Rogers, P. H. & Arnone, A. (2004). *Biochemistry*, **43**, 118–132.
Chan, N.-L., Rogers, P. H. & Arnone, A. (1998). *Biochemistry*, **37**, 16459–16464.
Forouhar, F. *et al.* (2007). *Proc. Natl Acad. Sci. USA*, **104**, 473–478.
Garman, E. F. (2010). *Acta Cryst.* D**66**, 339–351.
Kitagawa, T., Abe, M. & Ogoshi, H. (1978). *J. Chem. Phys.* **69**, 4516–4525.
Martínez-Ruiz, A., Cadenas, S. & Lamas, S. (2011). *Free Radic. Biol. Med.* **51**, 17–29.
Maxwell, J. C. & Caughey, W. S. (1976). *Biochemistry*, **15**, 388–396.
Mazzarella, L., Vergara, A., Vitagliano, L., Merlino, A., Bonomi, G., Scala, S., Verde, C. & di Prisco, G. (2006). *Proteins*, **65**, 490–498.
McGeehan, J. E., Carpentier, P., Royant, A., Bourgeois, D. & Ravelli, R. B. G. (2007). *J. Synchrotron Rad.* **14**, 99–108.
Merlino, A., Howes, B. D., Prisco, G., Verde, C., Smulevich, G., Mazzarella, L. & Vergara, A. (2011). *IUBMB Life*, **63**, 295–303.
Moncada, S., Palmer, R. M. & Higgs, E. A. (1991). *Pharmacol. Rev.* **43**, 109–142.
Murray, J. W., Garman, E. F. & Ravelli, R. B. G. (2004). *J. Appl. Cryst.* **37**, 513–522.
Opisov, A. N., Borisenko, G. G. & Vòladimirov, Y. A. (2007). *Biochemistry (Moscow)*, **44**, 259–292.
Otwinowski, Z. & Minor, W. (1997). *Methods Enzymol.* **276**, 307–326.
Owen, R. L., Pearson, A. R., Meents, A., Boehler, P., Thominet, V. & Schulze-Briese, C. (2009). *J. Synchrotron Rad.* **16**, 173–182.
Paithankar, K. S., Owen, R. L. & Garman, E. F. (2009). *J. Synchrotron Rad.* **16**, 152–162.
Santoro, F., Cappelli, C. & Barone, V. (2011). *J. Chem. Theory Comput.* **7**, 1824–1829.
Scholler, D. M., Wang, M.-Y. R. & Hoffman, B. M. (1979). *J. Biol. Chem.* **254**, 4072–4078.
Sheldrick, G. M. (2008). *Acta Cryst.* A**64**, 112–122.
Spiro, T. G. & Strekas, T. C. (1974). *J. Am. Chem. Soc.* **96**, 338–345.
Stong, J. D., Spiro, T. G., Kubaska, R. J. & Shupack, S. I. (1980). *J. Raman Spectrosc.* **9**, 312–314.
Suntsova, T. P., Beda, N. V. & Nedospasov, A. A. (2002). *IUBMB Life*, **54**, 281–292.
Szabo, A. & Barron, L. D. (1975). *J. Am. Chem. Soc.* **97**, 660–662.
Verde, C., Vergara, A., Mazzarella, L. & di Prisco, G. (2008). *Curr. Protein Pept. Sci.* **9**, 578–590.
Vergara, A., Franzese, M., Merlino, A., Bonomi, G., Verde, C., Giordano, D., di Prisco, G., Lee, H. C., Peisach, J. & Mazzarella, L. (2009). *Biophys. J.* **97**, 866–874.
Vergara, A., Franzese, M., Merlino, A., Vitagliano, L., Verde, C., di Prisco, G., Lee, H. C., Peisach, J. & Mazzarella, L. (2007). *Biophys. J.* **93**, 2822–2829.
Vergara, A., Merlino, A., Pizzo, E., D'Alessio, G. & Mazzarella, L. (2008). *Acta Cryst.* D**64**, 167–171.
Vergara, A., Vitagliano, L., Merlino, A., Sica, F., Marino, K., Verde, C., di Prisco, G. & Mazzarella, L. (2010). *J. Biol. Chem.* **285**, 32568–32575.
Vergara, A., Vitagliano, L., Verde, C., di Prisco, G. & Mazzarella, L. (2008). *Methods Enzymol.* **436**, 425–444.
Vitagliano, L., Vergara, A., Bonomi, G., Merlino, A., Verde, C., di Prisco, G., Howes, B. D., Smulevich, G. & Mazzarella, L. (2008). *J. Am. Chem. Soc.* **130**, 10527–10535.